CHAPTER - 16

FUNGI-MEDIATED SYNTHESIS OF SILVER NANOPARTICLES: CHARACTERIZATION PROCESSES AND APPLICATIONS

NELSON DURÁN[1], PRISCYLA D. MARCATO[1], AVINASH INGLE[2], ANIKET GADE[2] AND MAHENDRA RAI[2]

[1]*Instituto de Química, Biological Chemistry Laboratory, Universidade Estadual de Campinas, C.P. 6154, Campinas CEP 13083-970, S.P., Brazil*
E-mail: duran@iqm.unicamp.br
[2]*Department of Biotechnology, SGB Amravati University, Amravati-444 602, Maharashtra, India; E-mail: mkrai123@rediffmail.com, pmkrai@hotmail.com*

Introduction

The term "nanotechnology" is derived from the Greek word 'nano', meaning 'dwarf', and applies to the principles of engineering and manufacturing at a molecular level. The common definition of nanotechnology is that of manipulation, observation, measurement and synthesis at a scale of 1 to 100 nanometers (Raj and Asha, 2009). Nanobiotechnology is a new branch of science dedicated to the improvement and utilization of devices and structures ranging from 1 to 100 nm in size, in which new chemical, physical, and biological properties, not seen in bulk materials, can be observed. There is tremendous excitement in this field with respect to their fundamental properties, organization of superstructure and applications.

Nanomaterials exhibit a number of special properties; therefore, it may provide solutions to technological and environmental challenges in different areas like medicine, agriculture, solar energy conversions, catalysis and water treatment (Dahl *et al.*, 2007; Hutchison, 2008). Nanoparticles have a very high surface area to volume ratio, this provides a tremendous driving force for diffusion, especially at elevated temperatures and hence it plays an important role in field of drug delivery (Mah *et al.*, 2000).

The synthesis of metallic nanoparticles followed by a green-procedure is of great interest in the actual environmental concern. There are many production processes of silver nanoparticles but the biological one is playing an important role for avoiding the environmental pollution caused by physical and chemical procedures. Many reviews on the biosynthesis of metallic nanoparticles were already published showing the importance of these nanoparticles (Sastry *et al.*, 2003; Senapati *et al.*, 2004; Mandal *et al.*, 2006; Mohanpuria *et al.*, 2008; Bhattacharya and Mukherjee, 2008; Chen and Schluesener, 2008; Sharma *et al.*, 2009; Rai *et al.*, 2009).

Many fungi have been used to produce silver nanoparticles intracellularly or extracellularly. Several fungi were studied, such *as Verticillium* (Mukherjee *et al.*, 2001a), *Phoma sp* (Chen *et al.*, 2003; Birla *et al.*, 2009), *Phaenerochaete chrysosporium* (Vigneshwaran *et al.*, 2006), *Aspergillus niger* (Gade *et al.*, 2008), *Aspergillus fumigatus* (Bhainsa and D'Souza, 2006), *Aspergillus flavus* (Vigneshwaran *et al.*, 2007), *Fusarium oxysporum* (Ahmad *et al.*, 2003; Senapati *et al.*, 2004; Durán *et al.*, 2005; 2007), *Fusarium semitectum* (Basavaraja *et al.*, 2008), *Fusarium acuminatum* (Ingle *et al.*, 2008), *Fusarium solani* (Ingle *et al.*, 2009), *Penicillium* (Sadowski *et al.*, 2008), *Trichoderma asperellum* (Mukherjee *et al.*, 2008), *Coriolus versicolor* (Sanghi and Verma, 2009) and *Cladosporium cladosporioides* (Balaji *et al.*, 2009).

The present chapter focuses on various methods required for the characterization of silver nanoparticles, fungal species used for the synthesis of metal nanoparticles and application of nanoparticles in various fields including opto-electronics, medicine, biosensors, DNA labeling, etc.

Characterization

The silver nanoparticles can be characterized by different techniques such as Ultraviolet-Visible spectroscopy, fluorescence, fourier-transformed-infrared spectroscopy, X-ray diffraction, microscopy techniques, and photoluminescence spectra. These techniques can provide the information about the formation, size and morphology of the particles, capping, stability and other information as described in more detail below.

Ultraviolet-Visible Spectroscopy

The formation and stability of silver nanoparticles can be monitored by UV–Vis spectral analysis. Metallic nanoparticles smaller than or comparable to the penetration depth of electromagnetic fields in the metal have surface plasmon resonance. This phenomenon causes a strong absorption and scattering of visible and infrared light that explain the color of colloidal solutions of different metals (Krasovskii and Krasovskii, 2008). In the specific case of silver nanoparticles, the band in the UV-Vis spectrum corresponding to the surface plasmon resonance occurs at around 415-470 nm.

The plasmon absorption can be used to verify the formation of silver nanoparticles. The shape and position of plasmon resonance depends on a number of factors such as the dielectric constant of the medium, size and shape of the particles, surface-adsorbed species, etc. The Fig. 16.1 shows the UV-Vis spectrum of silver nanoparticles produced by *Fusarium oxysporum*. An increase in the plasmon absorption (ca. 420 nm) can be observed with time indicating the formation of silver nanoparticles formation. The maximum wavelength can vary with the size and the shape of silver nanoparticles. The maximum absorption is dislocated to larger wavelength with the decrease of particle size (Vigneshwaran *et al.*, 2006).

Silver nanoparticles with different size and shape can be produced by biological method depending on concentration of the Ag^+ ion in solution, the enzymes released by fungal strains and pH of the solution. The size and shape of particles are important factors in application of silver nanoparticles (He *et al.*, 2002; Balaji *et al.*, 2009).

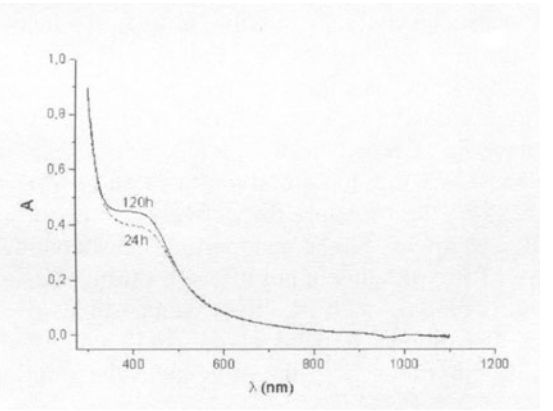

Fig. 16.1: UV-Vis spectra as a function of time of reaction of an aqueous solution of 10^{-3} M $AgNO_3$ with the fungal filtrate from *Fusarium oxysporum*.

Other important absorption band to silver nanoparticles is at 378 nm. This band appears as shoulder and corresponds to the transverse plasmon vibration in the silver nanoparticles while the peak at 420 nm is due to excitation of longitudinal plasmon vibrations. This band as well as the band around 420 nm indicates the formation of silver nanoparticles. The separation between the bands indicate that silver nanoparticles are formed mostly as aggregates (Basavaraja *et al.*, 2008).

The UV-Vis spectroscopy can be used to characterize the protein around the biosynthesized silver nanoparticles. The aromatic amino acids of protein present an absorption band at ca. 270 nm. This band is due to electronic excitations in tryptophan and tyrosine residues in the proteins. The interaction between protein and silver nanoparticles can also be studied by fluorescence and fourier-

transformed-infrared spectroscopy as described below (Ahmad *et al.*, 2003; Durán *et al.*, 2005).

Fluorescence

The fluorescence technique can characterize the interactions of protein-nanoparticle. When silver nanoparticles dispersion is excited in λ = 260 nm (maximum optical transitions in tryptophan and tyrosine residues of proteins), a band centered at ca. 340 nm appears. The nature of this emission band indicates that the proteins bound to the surface of nanoparticles and those present in the solution in the native form. Probably in the reduction process the tertiary structure of the proteins is not affected with the binding of silver nanoparticles to the surface (Ahmad *et al.*, 2003; Durán *et al.*, 2005).

Fourier-Transformed-Infrared spectroscopy (FTIR)

The FTIR spectroscopy is very important to characterize the protein binding with the silver nanoparticles and it is possible to quantify secondary structure in metal nanoparticle–protein interaction. The position of bands in the FTIR spectra from the amide I and II of proteins are sensitive indicator of conformational changes in the protein secondary structure (Gole *et al.*, 2001). The band in FTIR of amide I and amide II of native protein appears at around 1640 and around 1540 cm^{-1}. These bands are due to carbonyl stretch and –N–H stretch vibrations in the amide linkages of the proteins, respectively. Thus, the presence of these bands in the FTIR spectra of silver nanoparticles dispersion indicate that the secondary structure of the proteins is not affected during the formation of silver nanoparticles or by its binding with the silver nanoparticles (Balaji *et al.*, 2009). The FTIR spectra also shows a band at ca. 1450 cm^{-1} that corresponds to methylene scissoring vibrations from the proteins in the solution (Ahmad *et al.*, 2003).

FTIR also supply information about thiol derivatives surrounding the metallic cores giving more details about the protein capping to the silver nanoparticles. The –SH stretches in native protein occur at 2590–2540 cm^{-1}. The absence of the band in this region indicates the formation of a bond between the S atoms and silver clusters (chemisorption) (Tan *et al.*, 2002; Sanghi and Verma, 2009).

X-ray diffraction (XRD)

XRD is an important technique to evaluate the formation of silver nanoparticles and to determine the particle size. Silver nanoparticles produced by fungi showing a number of Bragg reflections corresponding to the (1 1 1), (2 0 0), (2 2 0) and (3 1 1) sets of lattice planes. These planes correspond to FCC structures of silver (index JCPDS file no. 03-0921). This result demonstrate crystalline nature of silver nanoparticles.

The size of silver nanoparticles can be calculated by Debye-Scherrer's equation:

$$D = (K\lambda)/ (\beta_{cor} \cos\theta), \text{ with } \beta_{cor} = (\beta^2_{sample} - \beta^2_{ref})^{1/2}$$

Where D is the average crystal size, K is the Scherrer's coefficient (0.89), λ is the X-ray wavelength (λ = 1.542 Å), θ Bragg's angle (2θ = 25.1°), β_{cor} the corrected of the full width at half-maximum (FWHM) in radians, β_{sample} and β_{ref} are the FWHM of the reference and sample peaks, respectively (Durán *et al.*, 2007). The diffraction signal in (111) plane of 2θ spectrum is used to calculate the silver nanoparticle size by Scherrer's equation.

In general, the calculated average particle size of the silver by XRD is also in line with the observation of the TEM results (Basavaraja *et al.*, 2008; Balaji *et al.*, 2009).

Transmission Electron Microscopy (TEM)

Morphology of silver nanoparticles can be observed by microscopic techniques such as TEM and SEM. TEM micrographs of nanoparticles can show whether the silver nanoparticles are symmetrical and with spherical shaped, whether the particles form aggregate or not and also determine the average size. Furthermore, it is possible to do the elemental analysis using the Elemental Spectroscopy Imaging (ESI). This analysis is very important to silver nanoparticles produced by microorganisms because it can characterize the stabilization by capping around the particles to confirm if fungal proteins are responsible for covering and stabilizing the particles or not (Vigneshwaran *et al.*, 2006; Duran *et al.*, 2007; Sanghi and Verma, 2009). TEM images can also be used to localize the silver nanoparticles in fungal or bacterial cell and this could be important to elucidate the mechanism of their formation or their antimicrobial activity, respectively (Mukherjee *et al.*, 2001b).

TEM under high resolution of a silver nanoparticles sample can analyze the nanoparticles preservation for long time. This led to observe the effect of ageing on the size of the nanoparticles. Furthermore, mean value of particle size can be estimated from the particle size histogram assuming a log-normal distribution of the particle diameter D according to the equation given below:

$$f(D) = (1/D\sigma\sqrt{2\pi}) \text{ [exp] } \{-[\ln(D/D_0)]^2/ 2\sigma^2\}$$

Where D_0 (15 nm) is the estimated median value for particle diameter and σ (0.1) is the distribution width (Mukherjee *et al.*, 2008).

Scanning Electronic Microscopy (SEM)

Morphology of silver nanoparticles and their elemental characterization can be made by SEM combined with Energy Dispersive X-ray Spectroscopy (EDS). The sample needs to be dried before its analysis by SEM because this technique is made under vacuum. But, high magnifications in ''wet mode'' can be made by

Environmental Scanning Electron Microscope (ESEM). This technique can be associated with a specially designed cooling stage, combined with energy diffraction analysis of X-rays (EDX) are used in some cases in silver nanoparticles determination in fungal cells. It is possible to be observed by ESEM silver nanoparticles on the surface of the mycelial mat when silver nanoparticles are formed in presence of fungal mycelium. The EDX coupled to ESEM allows the elemental analysis of isolated nanoparticles and particles on surface of fungal mycelium confirming the presence of these nanoparticles in the mycelium (Vigneshwaran *et al.*, 2006). Silver location of nanoparticles and their distribution on surface of the fungal cell can also be observed by SEM (Mukherjee *et al.*, 2001b; Vigneshwaran *et al.*, 2007).

SEM micrograph of silver nanoparticles shows, in many cases, aggregated particles due to the capping agent. Therefore, the particles size measured by SEM can be larger than the size measured by TEM or XRD (Durán *et al.*, 2005).

Photoluminescence

Photoluminescence is an effective method to evaluate the optical property of metallic nanoparticles as photonic materials. Silver nitrate solution does not show emission peak but the silver nanoparticles produced by fungus *Phanerochaete chrysosporium* showed an emission peak at 423 nm with very broad base. This result can be explained by the ability of silver nanoparticles to enhance the fluorescence emission intensity and photostability of nearby fluorophores. Therefore, the emission peak intensity at 423 nm of protein bound to silver nanoparticles might be increased (Vigneshwaran *et al.*, 2006). Curiously, the emission peak of silver nanoparticles produced by *Aspergillus flavus* was at 553 nm with very broad base, and no explanation for this big difference was provided (Vigneshwaran *et al.*, 2007).

Characterization of silver nanoparticles synthesized by fungi

Verticillium

Verticillium is a genus of fungi in the division Ascomycota. Within the genus, diverse groups are formed comprising saprophytes and parasites of higher plants, insects, nematodes and other fungi, thus it can be seen that the genus is a wide ranging group of taxa characterised by simple but ill-defined characters. The genus may be broadly divided into three ecologically based groups, (i) mycopathogens (ii) entomopathogens (Zare and Gams, 2001), and (iii) plant pathogens and related saprotrophs (Barbara and Clewes, 2003).

Recently, the genus has undergone some revision into which most entomopathogenic and mycopathogenic isolates fall into a new group called *Lecanicillium*. Plant pathogenic isolates still retain the original genus name *Verticillium*. The better known species of *Verticillium* are *V. dahliae* and *V. albo-*

atrum that cause a wilt disease called Verticillium -wilt in more than 300 dicot plant species (Zare and Gams, 2001).

Biotransformation of silver ions by *Verticillium* (Mukherjee *et al.*, 2001a), was monitored by visual inspection of the biomass as well as measurement of the UV-Vis spectra from the fungal cells and the aqueous medium in the reaction mixture. The silver nanoparticles in fungal mycelium were characterized by UV-Vis spectroscopy (Shimadzu dual-beam spectrophotometer-model UV-1601PC), X-ray diffraction (XRD- Leica Stereoscan-440), and scanning electron microscopy (SEM equipped with a Phoenix EDX attachment). The location of the silver nanoparticles in the *Verticillium* cells was investigated by transmission electron microscopy (TEM-JEOL Model 1200EX instrument operated at an accelerating voltage of 60 kV) through the thin sections of *Verticillium* cells after their exposition with Ag^{+} ions .

The UV-Vis spectra recorded from a biofilm of the fungal cells before and after immersion in silver ions showed that the fungal cells exposed to these ions showed absorbance at ca. 450 nm. The presence of the broad resonance peak indicated an aggregated structure of the silver particles in the film. The presence of uniformly distributed silver nanoparticles on the surface of the fungal cells by SEM was observed. The EDX spectrum recorded in the spot profile mode showed densely populated silver nanoparticle regions on the surface of the fungal cells. The TEM image showed small particles of silver organized on the mycelial wall as well as some larger particles within the cells (particle diameter of 25 ± 12 nm).

Phoma

Phoma is a genus of common coelomycetous soil fungi belongs to phylum Ascomycota. It contains many plant pathogenic species. About 200 *Phoma* taxa have been defined and recognized which may be divided into two large groups: (i) plurivorous fungi, generally saprobic or weakly parasitic, mainly from temperate regions in Eurasia, but occasionally also found in other parts of the world (including areas with cool or warm climates); and (ii) specific pathogens of cultivated plants (Van der Aa *et al.*, 1990).

Conidia are colorless and usually unicellular. The pycnidia are black and depressed in the tissues of the host (Rai and Rajak, 1985). *Phoma* is arbitrarily limited to those species in which the conidia are less than 15 μm as the larger conidial forms have been placed in the genus *Macrophoma*. The most important species include *Phoma exigua, P. glomerata, P. sorghina, P. multirostrata, P. medicaginis* and *P. betae*, etc.

Phoma sp. was used as producer of silver nanoparticles for the first time by Chen *et al.* (2003). The quality/quantity adsorption of silver nanoparticles in fungal mycelium was carried out using an atomic absorption spectrometer (AAS) (HITACHI Z-8000, Hitachi, Tokyo, Japan or SOLAAR-M6, Spectronic Unicam Ltd, Rochester, NY, USA). The size of Ag particles adsorbed on the mycelium

surface was observed and measured under TEM (HITACHI H-800). The surface atoms of silver particles on the mycelium were measured by XPS (XSAM800-Kratos, Manchester, UK).

According to the quality and quantity assay by atomic absorption spectrometer (AAS), each gram of dry mycelium produced around 13.4 mg of silver and the amount of Ag adsorbed was 13.9 $mg.L^{-1}$. This value was lower than other fungi like *Aspergillus terreus*. The lower adsorption capacity can be due to freeze-drying process used before the mycelium is exposed to silver ions.

The particles size measured by TEM was 71.06 ± 3.48 nm and this analysis showed a great number of tiny silver particles on mycelium. As per the XPS analyses and according to the standard (Ag_{3d} = 368.2 eV), it could be concluded that Ag^{+} was exactly reduced to Ag^{o}.

Another species of *Phoma* used for the synthesis of silver nanoparticles was *P. glomerata* (Birla *et al.,* 2009). In this study, the authors reported extracellular synthesis of silver nanoparticles when the fungal cell filtrate was treated with aqueous silver ions (silver nitrate 1mM) and incubated at room temperature. The silver nanoparticles synthesized were found to be in the range of 60-80nm when the colloidal solution of these silver nanoparticles was analyzed by using scanning electron microscopy (JEOL 6380A) (Mycelial growth of *P. glomerata* shown in Fig. 16. 2 A).

Further, Birla *et al.* (2009) evaluated the effect of silver nanoparticles in combination with commercially available antibiotics against human pathogenic bacteria viz. *E. coli, Pseudomonas aeruginosa* and *S. aureus* and reported that the antibacterial activities of ampicillin, gentamycin, streptomycin and vancomycin were enhanced in combination with silver nanoparticles against the Gram-negative micro-organisms, i.e. *E. coli* and *P. aeruginosa* as compared with *S. aureus*.

Phaenerochaete chrysosporium

Extracellular biosynthesis of silver nanoparticles by *Phaenerochaete chrysosporium* (a white-rot fungus) was reported by Vigneshwaran *et al.* (2006). The particles were characterized by UV–Vis spectroscopy (Specord 50 Analytikjena® spectrophotometer), X-ray diffraction analysis (Philips® automatic X-ray diffractometer with Philips® PW 1830 X-ray generator), scanning electron microscopy (Philips® XL 30 SEM at 10–17.5 kV), transmission electron microscopy (Philips® EM208 operating at 200 kV) and photoluminescence spectroscopy (Perkin-Elmer LS55® Spectrofluorimeter using 90° illumination). The particles exhibited the plasmon band at 470 nm. The particle size reduction shifts the plasmon band to larger wavelength. Thus, the plasmon band shift from 413 nm to 470 nm and the band was broad with an absorption tail in the longer wavelengths, which could be due to the size and shape distribution of the particles. The same conclusion was afforded with the XRD measurements. Fungal mycelium after challenged with silver ions was

analyzed by ESEM showing silver nanoparticles on the surface of the mycelial mat with size of approximate from 50 to 200 nm. The ESEM images indicate the reduction process being held on the surface. The TEM images showed particles not uniform size and shape with predominance pyramidal shape with different size. The photoluminescence spectra of silver nitrate solution treated with the fungus, showed an emission peak at 423 nm with very broad profile (fungal protein bound to nanoparticles).

Aspergillus niger

Aspergillus niger is one of the most common species of the genus *Aspergillus*. It causes a disease called black-mold on fruits and vegetables such as grapes, onions, and peanuts, and is a common contaminant of food. It is ubiquitous in soil and is commonly reported from indoor environments, where its black colonies can be confused with those of *Stachybotrys* (species of which have also been called "black mold") (Samson *et al.*, 2001).

Some strains of *A. niger* have been reported to produce potent mycotoxins called ochratoxins (Abarca *et al.*, 1994), but other sources disagree, claiming this report is based upon misidentification of the fungal species. Recent evidence suggests that *A. niger* strains do produce ochratoxin A (Samson *et al.*, 2001; Schuster *et al.*, 2002).

Extracellular biosynthesis of silver nanoparticles by *Aspergillus niger* isolated from soil has been reported by Gade *et al.* (2008). The UV-Vis spectra (Perkin Elmer, Labda-25) showed a band centered at 420 nm that increased with the time demonstrating the formation of silver nanoparticles. Furthermore, the color of fungal filtrate changed from dark-yellow to dark-brown which confirms the formation of nanoparticles (Bhainsa and D'Souza, 2006). Homogeny and spherical particles were observed by TEM (Carl Zeiss CEM-902 transmission electron microscope 80 KeV, equipped with a Castaing-Henry-Ottensmeyer energy filter spectrometer within the column). Elemental Spectroscopy Imaging (ESI) was carried out using monochromatic electrons corresponding to the sulfur L2,3-edge. The energy-selecting slit was set at 367 ± 6 keV for Ag and 165 ± 6 eV for S. The images were recorded by a Proscan high-speed slow-scan CCD camera and processed by AnalySis 3.0 system. In this analysis S and N atoms were observed around the silver nanoparticles indicating the association between the nanoparticles and fungal proteins. This protein capping around the particles are responsible for their stabilization by long periods. The protein was also characterized by fluorescence in similar way as previously published, where a fluorescence emission spectra of fungal filtrate exhibited a peak centered at 340 nm (Durán *et al.*, 2005).

TEM images were also used to study the antimicrobial effect of silver nanoparticles. TEM images showed the efficient antimicrobial effect of these particles that disrupted completely the cell membrane after 60 minutes. Furthermore, silver nanoparticles inside the bacteria were observed

demonstrating the capacity of silver nanoparticles to penetrate in to bacterial cell. Mycelial growth of *A. niger* is shown in Fig. 16.2 B.

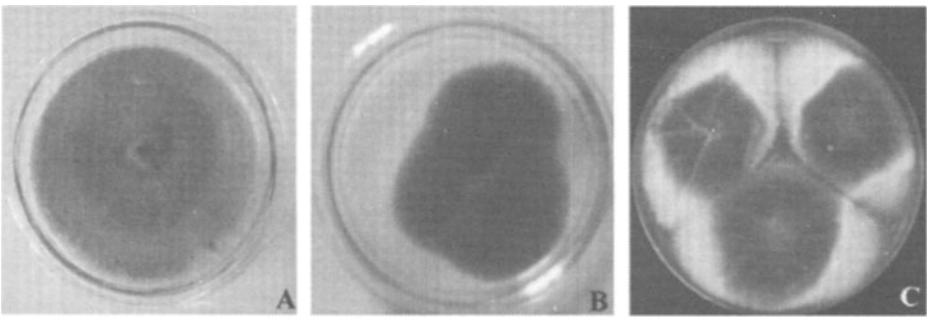

Fig. 16.2. Growth on PDA: (A) *Phoma glomerata* (B) *Aspergillus niger* and (C) *A. fumigatus*

Aspergillus fumigatus

A. fumigatus is a saprotrophic fungus that is widespread in nature, typically found in soil and decaying organic matter such as compost heaps, where it plays an essential role in carbon and nitrogen recycling. Colonies of the fungus produce thousands of minute grey-green conidia (2-3 μm) from conidiophores (Fig.16.2 C). Until recently, *A. fumigatus* was thought to reproduce only by asexual methods, as neither mating nor meiosis had ever been observed in the fungus. However, in 2008 it was shown for the first time that *A. fumigatus* possesses a fully functional sexual reproductive cycle, 145 years after its original description by Fresenius (O'Gorman *et al.*, 2008).

The fungus is capable of growth at 37°C (human body temperature), but can grow at temperatures up to 50°C, with conidia surviving at 70°C. It regularly encounters in self-heating compost heaps. The conidia are ubiquitous in the atmosphere and it is estimated that everybody inhales several hundred spores each day; typically, however, these are quickly eliminated by the immune system in healthy individuals. In immunocompromised individuals such as transplant patients and people with AIDS or leukaemia the fungus is capable of becoming pathogenic and causing a range of diseases generally termed aspergillosis (O'Gorman *et al.*, 2008).

Silver nanoparticles produced by a *Aspergillus fumigatus* (Bhainsa and D'Souza, 2006) were characterized by the absorbance in an UV–Visible spectrophotometer (UV–Vis UV4, UNIVAM Ltd., UK), by TEM (TECNAI 120 at a voltage of 120 kV) and by X-ray diffraction (XRD) using Phillips PW 1710. An increase in the surface plasmon resonance centered at ca. 420 nm was observed until 72 hours of reaction. This results indicated an increased number of particles formed. Nanoparticles with variable shape were observed by TEM. Most particles exhibited spherical morphology and occasionally with triangular shape. The particle-size was in the range 5-25 nm. XRD analysis confirmed the

formation of crystalline particles exhibiting four intense peaks in the whole spectrum of 2θ value. The four intense peaks observed in the spectrum agree to the Braggs's reflection of silver nanocrystals reported in literature

Aspergillus flavus

Aspergillus flavus belongs to Ascomycota (Fig. 16.3A). It is also a common mold in the environment, and can cause storage problems in stored grains. *A. flavus* is particularly common on corn and peanuts, as well as water damaged carpets, and is one of the several species of mold known to produce aflatoxin which cause acute hepatitis, immunosuppression and hepatocellular carcinoma. It can also be a human pathogen, associated with aspergillosis of the lungs and sometimes causing corneal, otomycotic, and nasoorbital infections. Many strains produce significant quantities of aflatoxin (Klich, 2007), a carcinogenic and acutely toxic compound. *A. flavus* spores are allergenic.

Aspergillus flavus is the second most common agent of aspergillosis, the first being *A. fumigatus*. *A flavus* may invade arteries of the lung or brain and cause infarction. Neutropenia predisposes to *Aspergillus* infection. It also produces a toxin (aflatoxin) which is one of the aetiological agents for hepatocellular cacinoma (Crawfold, 2005). It grows as a yellow-green mold in culture. It produces a distinctive conidiophore composed of a long stalk supporting as inflated vesicle. Conidiogenous cells on the vesicle produces conidia. Many strains of *A. flavus* exhibit a greenish fluorescence under UV light that is correlated with levels of aflatoxin production.

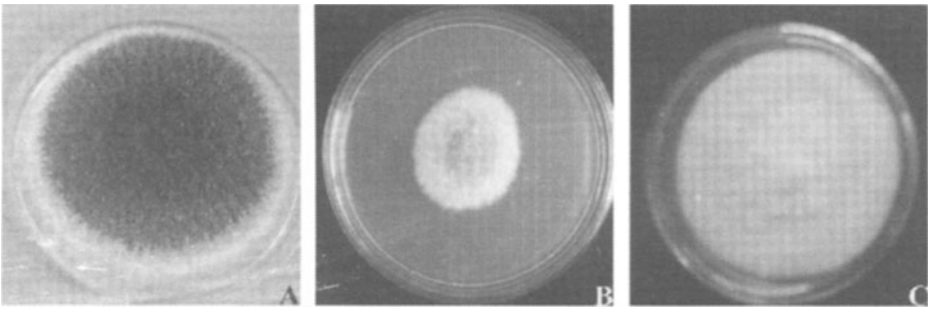

Fig. 16. 3. Growth on PDA: (A) *A. flavus* (B) *Fusarium oxysporum* and (C) *F. semitectum*

Biological synthesis of silver nanoparticles using *Aspergillus flavus* was studied by Vigneshwaran *et al.* (2007). The particles were analyzed by UV-Vis (Specord 50 ANALYTIKJENA® Spectrophotometer), by XRD (Philips® automatic X-ray Diffractometer with Philips® PW 1830 X-ray generator), by SEM (Philips® XL 30 SEM at 12–15 kV), by TEM (Philips® EM208 operating at 200 kV), FTIR (IRPrestige-21® Fourier Transform Infrared Spectrophotometer) and by photoluminescence spectra (Perkin Elmer LS55® Spectrofluorimeter using 90 illumination).

A characteristic surface plasmon absorption band at 420 nm was observed after 24 hours of reaction with maximum intensity in 72 hours. XRD analysis showed the planes of the face-centered cubic (FCC) silver (planes : 111, 200 and 220) referring to peaks in 38.5°, 44° and 64.5° in spectrum of 2θ, respectively. The XRD analysis of mycelium after exposure with silver ions exhibit more peaks due to the interaction of silver nitrate with fungal cell wall 2 matrix. Furthermore, broadening peaks was observed due to the small particle size of silver. The lattice constant calculated from this pattern was 4.087 Å, a value similar to the literature report. Isotropic nanoparticles (i.e., low aspect ratio) in shape and reasonably monodisperse were observed by TEM. Size particles, measured by TEM, were 8.92±1.61 nm and any agglomeration was observed. The SEM technique was used to characterize the fungal mycelium challenged with silver nitrate solution. SEM micrograph showed silver nanoparticles deposited in the fungal mycelium. The diffraction pattern confirmed the face-centered cubic 'FCC' crystalline structure of metallic silver.

The FTIR analysis confirmed the presence of protein in the samples of silver nanoparticles. An emission peak with very broad base in 523 nm was observed in photoluminescence spectra as fungal protein bound to silver nanoparticles.

Fusarium species

Fusarium is one of the most important genera of plant pathogenic fungi and widely distributed on plants and in soil. It also causes infection in animals and human beings. *Fusarium* species are responsible for wilts, blights, root-rots, and cankers in coffee, pine trees, wheat, corn, rice, carnations and grasses leading to the great economic losses (Hocking, 1987; Knoll *et al.*, 2002; Miller, 2002). *Fusarium* sp. grow rapidly on simple media like Potato dextrose agar (PDA) and Sabouraud dextrose agar (SDA) at 25°C and produce woolly to cottony, flat, spreading colonies. From the front, the colour of the colony may be white, cream, tan, salmon, cinnamon, yellow, red, violet, pink, or purple. From the reverse, it may be colorless, tan, red, dark purple, or brown. Microscopically *Fusarium* can be easily identified by its curve shaped and septate macroconidia which is its important characteristics. While hyaline septate hyphae, conidiophores, phialides, and microconidia are observed microscopically. In addition to these basic elements, chlamydospores are also produced in some species (Seifert, 1996).

Fusarium species have been extensively studied for their potential towards the synthesis of metal nanoparticles and therefore their morphology has been discussed in detail in this chapter.

Fusarium oxysporum

Fusarium oxysporum is the most widely dispersed of the *Fusarium* species and can be recovered from most soil of the regions and also found in association with many important crop plants. It causes *Fusarium* wilt disease in more than a hundred species of plants. It does so by colonizing the water-conducting vessels

(xylem) of the plant. As a result of this blockage and breakdown of xylem, symptoms appear in plants such as leaf wilting, yellowing and eventually plant death. Most commonly it is the causative agent of Panama disease of Banana (Fig. 16.3 B).

Morphologically the colonies of *F. oxysporum* on PDA varies widely. Mycelia may be floccose, sparse or abundant and range in color from white to pale violet. Abundant pale-orange or pale-violet macroconidia are produced in a central spore mass in some isolates. Small pale-brown, blue to blue-black or violet sclerotia may be produced abundantly by some other isolates. *F. oxysporum* usually produces a pale to dark-violet or dark-magenta pigments in the agar but some isolates produce no pigment at all. Some isolates of *F. oxysporum* mutate readily to the pionnotal form or to a flat "wet" mycelial colony with a yellow to orange appearance when cultured on PDA (Seifert, 1996).

The critical morphological features of *F. oxysporum* include the production of microconidia in false heads on short phialides formed on the hyphae, the production of chlamydospores and the shape of the macroconidia and the microconidia (Seifert, 1996).

The production of silver nanoparticles by *Fusarium oxysporum* was studied by UV-Vis spectroscopy (Shimadzu dual-beam spectrophotometer-model UV-1601 PC (Ahmad *et al.*, 2003; Senapati *et al.*, 2004) showed a strong surface plasmon resonance centered at ca. 413 nm.. Absorption band in low wavelength (ca. 270 nm) was observed and it was attributed to aromatic amino acids of proteins (tryptophan and tyrosine residues). This band indicates the release of proteins into solution by *F. oxysporum* and suggested the influence of protein in silver ions reduction (Durán *et al.*, 2005).

Through fluorescence spectroscopy (Perkin-Elmer LS 50B luminescence spectrophotometer) showed an emission band centered at ca. 340 nm indicating that the proteins bound to the nanoparticle and those present in the solution exist in the native form. This result was confirmed by FTIR (Shimadzu FTIR-8201 PC instrument) by the presence of three bands at 1650 cm^{-1}, 1540 cm^{-1} and 1450 cm^{-1}. The bands at 1650 and 1540 cm^{-1} referring to amide I and II of protein indicate that the secondary structure of the proteins was not affected in the silver ions reduction process. The silver nanoparticles observed by TEM (JEOL 1200EX instrument at a voltage of 80 kV) showed individual and aggregated silver particles. The particle morphology was spherical and occasionally triangular one with size of 5-50 nm. Crystalline silver particles were obtained as verified by diffraction pattern (X-ray diffraction-XRD), which was carried out in the transmission mode on a Philips PW 1830 instrument operating at 40 kV. The particle size measured by XRD using Debye-Scherrer's equation 7 nm. Similar results were obtained by Durán *et al.* (2005). In this work silver nanoparticles produced by *F. oxysporum* exhibited plasmon absorbance at 420 nm in the UV-Vis analysis (Agilent 8453—diode array) and size, measured by SEM (Jeol – JSM-6360LV), of 20-50 nm. TEM (Carl Zeiss CEM-902 transmission electron

microscope at 80 KeV) images of particles produced by the same fungus showed spherical particles with size of 1.6 nm calculated by XRD (XRD, model XD3A from Shimadzu) and the Scherrer's equation (Durán *et al.*, 2007). These nanoparticles were analyzed by elemental spectroscopy imaging (ESI) showing that the nanoparticles were formed by silver and the presence of the N and S atoms around the silver nanoparticles. This result was associated with the particle stabilization by the fungal proteins.

Fusarium semitectum

Fusarium semitectum is commonly isolated from soil and from diverse aerial plant parts in tropical and sub-tropical areas, *e.g.*, banana fruits and palm fronds, but it can also be recovered from soils in the arctic and deserts. Although there are many reports of *F. semitectum* being implicated in various diseases it is often not regarded as an important plant pathogen. It has been reported to cause a canker of walnut, pod and seed-rot of beans, reduced seed germination and seedling growth of sorghum, corky-dry-rot of melons, and storage rot problems of mushrooms (Seifert, 1996) .

Cultures usually grow rapidly and produce abundant dense aerial mycelia which are initially off-white and become reddish or brown with age (Fig. 16.3 C). Brown pigments may also be produced in the agar. Light-orange sporodochia may be produced by some strains.

The silver nanoparticles were synthesized by *F. semitectum* (Basavaraja *et al.*, 2008) and this production was followed by UV–Vis spectroscopy measurements (Elico spectrophotometer). The particles were characterized by XRD measurements (Siemens X-ray diffractometer (Japan)), TEM (Technai-20 Philips transmission electron microscope operated at 190 keV), and FTIR (Perkin-Elmer FT-IR Spectrum ONE).

The UV-Vis analysis confirmed the silver nanoparticles production by the surface plasmon resonance band at 420 nm. Silver nanoparticles formation was also confirmed by XRD, diffraction signals to corresponding facets of silver (1 1 1, 2 0 0, 2 2 0 and 3 1 1). The average particles size was calculated by XRD using the diffraction signal in 1 1 1 plane and the Scherrer's equation giving 35 nm. These particles were analyzed by TEM showing particles polydisperse and in spherical shape. From the FTIR analysis it was observed that the dispersion in the protein is due to the presence of bands referring to amide I and amide II and linkages of the proteins.

Fusarium acuminatum

Fusarium acuminatum found in temperate regions usually as a soil saprophyte or associated with roots and crowns of plants. It can occasionally be associated with root and crown diseases of a variety of hosts, especially legumes, and has been recovered from cereal grains in Canada, Europe, India and the

former Soviet Union. Recently, it has been reported that *F. acuminatum* can produce traces of mycotoxins like trichothecenes.

It is a relatively slow-growing species that produces white mycelium which is abundant in some isolates (Fig. 16.4 A). The mycelium is floccose with rose to burgundy pigmentation that can be grayish rose at the periphery. Sporodochia formed in the center of the colony in a small central spore mass and are pale-orange to dark brown. Red pigments (sometimes brown) are formed in the agar (Seifert, 1996).

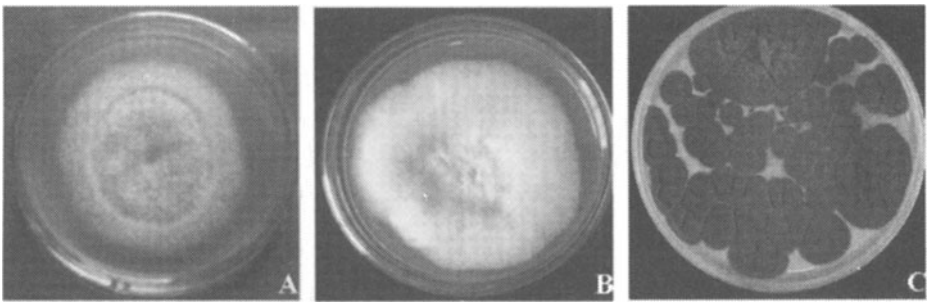

Fig. 16.4. Growth on PDA: (A) *F. acuminatum* (B) *F. solani* and (C) *Penicillium* sp.

Extracellular mycosynthesis of silver nanoparticles by *Fusarium acuminatum* Ell. and Ev. was reported in the literature (Ingle *et al.*, 2008). Plasmon resonance band was observed at 420 nm in the UV-Vis spetrum Perkin-Elmer - lambda-25). After 15-20 minutes of reaction with silver ions the dispersion color changed from yellowish to brown indicating the silver nanoparticles formation. These particles were analyzed by TEM (Phillips, CM12) operating at 120KV. TEM images showed spherical and polydisperse particles in the range of 5-40 nm. The particle size distribution histogram determined by TEM showed the large variation in the particle size with about 30% of the particles in the range of 0-5 nm and 7% in 40-45 nm ranges.

Fusarium solani

Fusarium solani is commonly distributed in soil and on plants. It causes onion-rot disease and also found associated with other crop plants and food grains. *F. solani* is, however, well documented as a pathogen of a number of legumes and other tropical plants where it is often associated with cankers and die-back problems of trees. Some economically important plants with significant diseases caused by *F. solani* includes, beans, citrus, cowpea, orchids, peas, peppers and potato.

It is most resistant species to the commercially available antifungal agent. With respect to human pathogenicity, *F. solani* has been recovered from eyes, nails and skin, bone, nasal cavities, infected wounds, and systemically infected cancer and HIV patients. Patients with keratitis resulting from infection with *F.*

solani were more likely to be HIV positive. *F. solani* may also cause endocarditis and lung disease, and has been shown to be allergenic (Seifert, 1996).

Cultures of *F. solani* usually are white to cream with sparse mycelium (Fig. 16.4 B). Sporodochia often are produced in abundance and may be cream, blue or green. Many isolates do not produce pigments in the agar although some violet or brown pigments may be observed.

F. solani isolated from infected onion was used for the biosynthesis of silver nanoparticles (Ingle *et al.*; 2009), silver nanoparticles produced were characterized by UV-Vis spectrophotometer (Perkin-Elmer-lambda-25), the UV-Vis spectrum showed a absorption peak at 420 nm and the FTIR (Perkin-Elmer) analysis carried out provides the evidence for the presence of proteins which helps for the stabilization by capping to the nanoparticles. TEM (Phillips, CM12) micrographs showed the production of spherical nanoparticles in the range of 5-35 nm with average size diameter of 16.32 nm.

Penicillium sp.

Penicillium is a mold that is widely distributed in nature, and is often found living on food and in indoor environments (Fig. 16.4C). The main species of *Penicillium* are *P. chrysogenum* and *P. notatum* (Samson *et al.*, 1977). It has rarely been reported as a cause of human disease. It is the source of several β-lactam antibiotics, most significantly penicillin. Other secondary metabolites of *P. chrysogenum* include various different penicillins, roquefortine C, meleagrin, chrysogine, xanthocillins, secalonic acids, sorrentanone, sorbicillin, and PR-toxin (de Hoog *et al.*, 2000).

Like many other species of the genus *Penicillium*, *P. chrysogenum* reproduces by forming dry chains of spores (or conidia) from brush-shaped conidiophores. The conidia are typically carried by air currents to new colonisation sites. In *P. chrysogenum* the conidia are blue to blue-green, and the mold sometimes exudes a yellow pigment. However, *P. chrysogenum* cannot be identified based on colour alone. Observations of morphology and microscopic features are needed to confirm its identity.

The airborne spores of *P. chrysogenum* are important human allergens. Vacuolar and alkaline serine proteases have been implicated as the major allergenic proteins (Shen *et al.*, 2003). *P. chrysogenum* has been used industrially to produce penicillin and xanthocillin X, to treat pulp mill waste, and to produce the enzymes polyamine oxidase, phospho-gluconate dehydrogenase, and glucose oxidase (de Hoog *et al.*, 2000; Shen *et al.*, 2003).

Penicillium strain isolated from soil (Sadowski *et al.*, 2008) produced silver nanoparticles which were monitored by UV-Visible spectrophotometer (HELIOS λ, ThermoElectron Corp.). The particles size was measured by laser diffractometry using a Mastersizer 2000 instrument (Malvern) equipped with HydroMu dispersing unit (Malvern) and the zeta potential was carried out using a Zetasizer Nano ZS (Malvern) and a titrator MPT-2.

Two bands were observed in the UV-Vis spectrum. The first one was a shoulder at 370 nm and the second was a band at 440 nm corresponding to excitation of transversal and longitudinal plasmon vibration in silver nanoparticles, respectively. Polydispersity of particles was observed by laser diffraction. The size was in the range of 100 nm until micrometers. This result was confirmed by SEM. The SEM micrograph of silver nanoparticles dried showed particles agglomerated. This polydispersity can be due to the drying process made before analysis in laser diffraction and SEM. The nanoparticles obtained exhibit negative zeta potential and this potential changed drastically from pH 2 to pH 8 presenting isoelectric point in pH below 2. In acid pH the particles were instable but in pH > 8 the particles were stable due to the electrostatic repulsion.

Trichoderma asperellum

Trichoderma species are present in soil, where they are the most prevalent culturable fungi. Many species in this genus can be characterized as opportunistic avirulent plant symbionts (Harman *et al.*, 2004).

Cultures are typically fast growing at 25-30°C, but do not grow above 35°C. Colonies at first appear transparent on media such as cornmeal dextrose agar (CMD) or white on richer media such as potato dextrose agar (PDA). Mycelium typically not obvious on CMD, conidia typically forming within one week in compact or loose tufts in shades of green or yellow or less frequently white. Yellow pigment may be secreted into the agar, especially on PDA. A characteristic sweet or 'coconut' odor is produced by some species (Harman *et al.*, 2004).

Several strains of *Trichoderma* have been developed as biocontrol agents against fungal diseases of plants. The various mechanisms include antibiosis, parasitism, inducing host-plant resistance, and competition. Most biocontrol agents are from the species *T. harzianum, T. viride*, *T. hamatum* and *T. asperellum*. The biocontrol agent generally grows in its natural habitat on the root surface, and so affects root disease in particular, but can also be effective against foliar diseases (Harman, 2006).

Trichoderma asperellum were used to produce the silver nanoparticles (Mukherjee *et al.*, 2008). The bioproduction was detected by UV-Vis spectrophotometer (JASCO double-beam UV–Vis spectrophotometer model V-530); the particles were characterized by XRD (Philips X'pert Pro XRD unit); by Transmission electron microscopy and selective area electron diffraction (SAED) (JEOL 2000 .FX machine); by FTIR at room temperature (JASCO FTIR spectrometer model No. 4100). Furthermore, the silver nanoparticles were analyzed by macro-Raman set-up using 532 nm line of a diode laser for excitation, 0.9 m single-stage monochromator to the scattered light and a CCD detector. The particle size was measured by dynamic light-scattering (DLS) using 532 nm line of a He–Ne laser as the source for excitation.

The silver nanoparticles exhibited an intense peak at 410 nm corresponding to the surface plasmon resonance. The particles size, calculated by XRD applying Scherrer's equation was 17 nm and the XRD pattern exhibited a broad and intense peak at 38.4° and a hump at 64.5°. These peaks corresponding to diffraction from the (111) and (220) planes of silver with "FCC" lattice. The broadening of the peaks indicates that the particles are in the nanometric range. This result was confirmed by selected-area electron diffraction pattern. In this analysis was observed concentric rings referring to (111), (311) and (220) planes of silver. The particles size, measured by TEM, was in the range 13–18 nm.

After 6 month, the silver nanoparticles size was measured by DLS showing 35.4 nm. This value is larger than size measured by XRD and TEM because in DLS analysis is considerate in the size of the hydrated capping agents (proteins) and the solvation effects. Thus, the hydrodynamic diameter determinated by DLS (could be as high as 1.2 times the original diameter of the capped particles).

FTIR spectroscopic studies together with Raman spectrum gave the data to establish the silver nanoparticles biosynthetic mechanism and the nature of the capping species identified. Raman analysis showed selective enhancement of certain chemical bond vibrations in organic moieties (the capping agents) associated with the silver particles that extends the feasibility of using these nanoparticles as potential templates for surface enhanced resonance Raman spectroscopy (SERS).

Coriolus versicolor

A controlled and up-scalable method to produce silver nanoparticles mediated by *Coriolus versicolor* was published (Sanghi and Verma, 2009). The nanoparticles were characterized by UV/Vis Spectrophotometer (Perkin Elmer, USA), Infrared (IR) using reflectance mode (BRUCKER, VERTEX-70), XRD (ARL X TRA X-ray Diffractometer). The fungal mycelium with and without silver nanoparticles was dried and after analyzed by XRD. The particles were also characterized by TEM (Philips - EM208 operating at 200 kV) and Atomic force microscopy (AFM) (PicoscanTM Molecular imaging, USA).

The absorption spectrum showed the band centered at 430 nm and this band was blue shifted to 420 nm when the pH was changed to 10 indicating the decrease particle size. By the XRD analysis was observed the diffraction peaks corresponding to facets of silver (111, 200, 311) indicating the formation of crystalline silver nanoparticles. Furthermore, the XRD pattern of fungal mycelium after exposition with silver ions showed more diffraction peaks referring to Ag_2S ($2\theta = 33.3°$, $39.2°$, $46.2°$), Ag_3O_4 ($2\theta = 32.09°$), AgO ($2\theta = 46.0°$) and peaks corresponding to silver ions ($2\theta = 55°$, $65.5°$, $68.8°$).

FTIR gave information regarding silver nanoparticles formation mechanism and composition of thiol derivatives surrounding the metallic cores. After silver nanoparticles produced was observed a new band in 1735 cm^{-1} referring to carbonyl stretch vibrations in ketones, aldehydes and carboxylic acids. This result

indicates that the reduction of the silver ions is coupled to the oxidation of the hydroxyl groups in fungal mycelium molecular and/or its hydrolysates. Also was observed in the FTIR spectrum the ν SH stretches (2590–2540 cm^{-1}). After the reaction, at alkaline pH, the band at 2526 cm^{-1} completely disappears indicating the formation of a bond between the S atoms and silver clusters (Ag-S bond). Silver nanoparticles spherical and symmetrical with size of 10 nm and without aggregation were observed by TEM. Besides, by TEM, agglomerated particles were observed when the pH was changed showing the influence of pH in the silver nanoparticles formation.

Cladosporium cladosporioides

Extracellular biosynthesis of silver nanoparticles was studied using the fungus *Cladosporium cladosporioides* (Balaji *et al.*, 2009). Silver nanoparticles were analyzed by UV-Vis, TEM (Technai-20 Philips transmission electron microscope operating at 190 keV), XRD (Siemens X-ray diffractometer), FTIR (PerkinElmer FT-IR Spectrum ONE at a resolution of 4 cm^{-1}).

UV–Vis spectrum showed the band corresponding to the surface plasmon resonance at 415 nm indicating the silver nanoparticles formation. Besides, size, calculated by Scherrer's equation was 35 nm. This value was in agreement with TEM results. The TEM image showed polydisperse and spherical particles with size in the range of 10-100 nm. The bands corresponding to amide I and amide II from proteins was identified in the FTIR spectrum confirmed the presence of protein that can bind to silver nanoparticles stabilizing these particles in the medium.

Multiple applications of metal nanoparticles

Metal nanoparticles have many physicochemical and optoelectronic properties. Due to all diverse properties, nanoparticles have multiple applications in various fields like electronics, agriculture and medicine. Some of the nanoparticles that can be produced by fungi may be of particular relevance to new and emerging technologies. The use of silver coatings in solar absorption systems has already been mentioned. Other applications in such areas include the use of gold nanoparticles as precursors to coatings for electronic applications (Mukherjee *et al.*, 2001a) and platinum nanoparticles in the production of fuel cells (Riddin *et al.*, 2006).

The application in the field of medicine includes the formulations of many potential antimicrobial agents, which are effective against many human pathogens including multidrug-resistant bacteria (Ingle *et al.*, 2008). Ingle *et al.* (2008) evaluated the biosynthesized silver nanoparticles from *F. acuminatum* for their broad spectrum antibacterial activity on different human pathogens. The authors reported efficient antibacterial activity of silver nanoparticles against multidrug resistant and highly pathogenic bacteria such as *Staphylococcus aureus*, *Staphylococcus epidermidis*, *Salmonella typhi* and *Escherichia coli*.

Silver nanoparticles showed large antimicrobial effect than silver ions (1.4-1.9 folds). The maximum antibacterial activity of silver nanoparticles was against *Staphylococcus aureus* (17 mm), followed by *Staphylococcus epidermidis*, *Salmonella typhi* and the minimum by *E. coli* (10 mm). This result demonstrated that specific efficiency of silver nanoparticles can be related with differences from strain, which can be due the bacterial membrane structure. However, it warrants further investigation.

Sondi and Sondi (2004) reported antimicrobial activity of silver nanoparticles against *E. coli* as a model for Gram-negative bacteria. From the SEM micrographs, formation of aggregates composed of silver nanoparticles and dead bacterial cells were observed. It was also observed that the silver nanoparticles interact with the building elements of the bacterial membrane and cause damage to the cell. The TEM analysis and EDAX study confirmed the incorporation of silver nanoparticles into the membrane, which was recognized by formation of pits on the cell surface. They concluded that nanomaterials could prove to be simple, cost effective and suitable for formulation of new type of bacterial materials.

Another application of silver nanoparticles is the production of sterile materials. Cotton fabrics incorporated with 2% of silver nanoparticles produced by *F. oxysporum* (Durán *et al.*, 2007), exhibited high antibacterial effect against *S. aureus* (99.9% bacterial reduction). The fabrics, after the antibacterial assay, were analyzed by SEM-EDS showing the presence of the silver peak and the absence of the contamination with bacteria. These results demonstrated that silver nanoparticles can be used to turn sterile fabrics. Furthermore, the silver nanoparticles dispersion will be reused for impregnation of other fabrics, for example, working in a closed circuit causing less damage to the environment.

Kim *et al.* (2007) investigated the antimicrobial activity of silver nanoparticles against *E. coli* and *S. aureus* on Mullar Hinton agar plates. In this study yeast and *E. coli* were inhibited at low concentration of silver nanoparticles, where as the growth inhibitory effects on *S. aureus* were mild. Shahverdi *et al.* (2008) studied the activity of silver nanoparticles against *E. coli* and *Staphylococcus aureus*. Duran *et al.* (2007) used the silver nanoparticles in the preparations of cotton fabrics and also evaluated its activity against *S. aureus*. Rai *et al.* (2009) suggested that the silver nanoparticles produced by the fungi are the novel and new generation of antimicrobials.

Edelstein *et al.* (2000) developed the Bead ARray Counter (BARC) as a multi-analyte biosensor from nanoparticles which are used in DNA hybridization, magnetic microbeads, and giant magnetoresistive (GMR) sensors for the detection and identification of biological warfare agents. De La Isla *et al.* (2003), cover teeth surfaces with nanohybrid coatings containing an inorganic ceramic and an organic copolymer constituents. They reported the first ever values of scratch penetration depth and scratch recovery for bare and coated teeth. The authors found that uncoated teeth undergo viscoelastic recovery (healing) after microscratching, the first manifestation of bone viscoelasticity in tribology. The

coatings fill "valleys" in teeth surfaces. They concluded that improvement in the scratch resistance increases as compared to uncoated teeth is seen.

Cai *et al.* (2005) reported the nanotube spearing approach, in which they used nickel embedded carbon nanotubes coated with DNA. They further reported that when the nanotubes were introduced in the cells in presence of specially oriented magnetic field, the nanotubes align with the magnetic flux lines as they are pulled towards the cells. This enables the nanotubes to spear the cells, pass through the membrane and deliver the targeted DNA.

Final remarks

The most important methodology for silver nanoparticles synthesized by fungi was discussed and from this information it was possible to deduce that the control size and reactivity of silver nanoparticles caped with protein are quite different. The characterization of silver nanoparticles is very important to understand the mechanism of formation of these particles and its application. Several techniques can be used to analyze these particles such as UV-Vis spectroscopy, microscopy techniques, diffraction X-ray, fourier-transformed-infrared spectroscopy, fluorescence and photoluminescence. The reports of production of the nanoparticles are numerous, but the applications are still under study. The importance of protein on the surface of silver nanoparticles is still an open question. Further, it is also important to investigate whether different fungi have different proteins or not?.

References

Abarca, M., M. Bragulat, G. Castellá and F. Cabañes (1994). Ochratoxin A production by strains of *Aspergillus niger* var. *niger, Appl Environ Microbiol* 60 (7): 2650–2652.

Ahmad, A., P. Mukherjee, S. Senapati, D. Mandal, M. I. Khan, R. Kumar and M. Sastry (2003). Extracellular biosynthesis of silver nanoparticles using the fungus *Fusarium oxysporum*, *Colloids and Surfaces B: Biointerfaces* 28: 313-318.

Balaji, D.S., S. Basavaraja, R. Deshpande, D. Bedre, M.B.K. Prabhakar and A. Venkataraman (2009). Extracellular biosynthesis of functionalized silver nanoparticles by strains of *Cladosporium cladosporioides* fungus, *Colloids and Surfaces B: Biointerfaces* 68: 88-92.

Barbara, D.J. and E. Clewes (2003). Plant pathogenic *Verticillium* species: how many of them are there?, *Molecular Plant Pathology* 4(4): 297-305.

Basavaraja, S., S.D. Balaji, A. Lagashetty, A.H. Rajasab and A. Venkataraman (2008). Extracellular biosynthesis of silver nanoparticles using the fungus *Fusarium semitectum, Materials Research Bulletin* 43: 1164-1170.

Bhainsa, K.C. and S.F. D'Souza (2006). Extracellular biosynthesis of silver nanoparticles using the fungus *Aspergillus fumigatus, Colloids and Surfaces B: Biointerfaces* 47: 160-164.

Bhattacharya, R and P. Mukherjee (2008). Biological properties of "naked" metal nanoparticles, *Advanced Drug Delivery Reviews* 60: 1289-1306.

Birla, S.S., V.V. Tiwari, A.K. Gade, A.P. Ingle, A.P. Yadav and M.K. Rai (2008). Fabrication of silver nanoparticles by *Phoma glomerata* and its combined effect against *Escherichia coli*, *Pseudomonas aeruginosa* and *Staphylococcus aureus*, *Letters in Applied Microbiology* 48: 173-179.

Cai, D., J.M. Mataraja, Z.H. Quin, Z. Huang, J. Huang and T.C. Chiles. (2005). Highly efficient molecular delivery into mammalian cells using carbon nanotubes spearing, *Nat Methods* 2:449-454.

Chen, X. and H.J. Schluesener (2008). Nanosilver: A nanoproduct in medical application, *Toxicology Letters* 176: 1-12.

Chen, J.C., Z.H. Lin and X.X. Ma (2003). Evidence of the production of silver nanoparticles via pretreatment of *Phoma* sp.3.2883 with silver nitrate, *Letters in Applied Microbiology* 37: 105-108.

Crawford, J.M. (2005). *Liver and Biliary Tract.* Pathologic Basis of Disease, ed. Kumar V, Philadelphia: Elsevier Saunders. p. 924

Cui, C.B. (1996). Spirotryprostatin B, a novel mammalian cell cycle inhibitor produced by *Aspergillus fumigatus*, *Journal of Antibiotics* 49: 832–835.

Dahl, J., B.L. Maddux and J.E. Hutchison (2007). Toward Greener Nanosynthesis, *Chem Rev* 107: 2228-2269.

De la Isla, A., W. Brostow, B. Bujard, M. Estevez, J.R. Rodriguez and S. Vargas (2003). Nanohybrid Scratch Resistant Coating for Teeth and Bone Viscoelasticity Manifested in Tribology, *Mat Resr Innovat* 7:110-114.

Durán, N., P.D. Marcato, O.L. Alves, G.I.H. De Souza and E. Esposito (2005). Mechanistic aspects of biosynthesis of silver nanoparticles by several *Fusarium oxysporum* strains, *Journal of Nanobiotechnology* 3: 1-7.

Durán, N., P.D. Marcato, G.I.H. De Souza, O.L. Alves and E. Esposito (2007). Antibacterial effect of silver nanoparticles produced by fungal process on textile fabrics and their effluent treatment, *Journal of Biomedical Nanotechnology* 3: 203-208.

Edelstein, R.L., C.R. Tamanaha, P.E. Sheehan, M.M. Miller, D.R. Baselt and L.J. Whitman (2000). The BARC Biosensor Applied to the Detection of Biological Warfare Agents, *Biosensors Bioelectron* 14:805-813.

Gade, A.K., P. Bonde, A.P. Ingle, P.D. Marcato, N. Durán and M.K. Rai (2008). Exploitation of *Aspergillus niger* for synthesis of silver nanoparticles, *Journal of Biobased in Materials and Bioenergy* 2: 243-247.

Gole, A., C. Dash, V. Ramakrishnan, S.R. Sainkar, A.B. Mandale, M. Rao and M. Sastry (2001). Pepsin–gold colloid conjugates: Preparation, characterization, and enzymatic activity, *Langmuir* 17:1674-1679.

Harman, G.E., C.R. Howell, A. Viterbo, I. Chet and M. Lorito (2004). *Trichoderma* species-opportunistic avirulent plant symbionts, *Nature Reviews Microbiology* 2: 43–56.

Harman, G.E. (2006). Overview of mechanisms and uses of *Trichoderma* spp., *Phytopathology* 96: 190–194

Harshberger, J.W. (1917). A Text book of Mycology and Plant Pathology. Original from the University of Michigan: P. Blakiston's son and co. pp.261-262.

He, R., X. Qian, J. Yin and Z. Zhu (2002). Preparation of polychrome silver nanoparticles in different solvents, *Journal of Materials Chemistry* 12: 3783–3786.

Hocking, A.D. and S. Andrews (1987). Dichloran chloramphenicol peptone agar as an identification medium for *Fusarium* species and some dematiaceous hyphomycetes, *Transactions of the British Mycological Society.* 89: 239-244.

Hutchison, J.E (2008). Greener Nanoscience: A Proactive Approach to Advancing Applications and Reducing Implications of Nanotechnology, *ACS Nano* 2: 395-402.

Ingle, A., A. Gade, S. Pierrat, C. Sönnichsen and M. Rai (2008). Mycosynthesis of silver nanoparticles using the fungus *Fusarium acuminatum* and its activity against some human pathogenic bacteria, *Current Nanoscience* 4: 141-144.

Ingle, A., A. Gade, M. Bawaskar and M. Rai (2009). *Fusarium solani:* A novel biological agent for the extracellular synthesis of silver nanoparticles, *Journal of Nanoparticle Research.* (Doi: 10.1007/s11051-008-9573-y).

Kim, J.S., E. Kuk, K.N. Yu, J.H. Kim, S.J. Park and H.J. Lee (2007). Antimicrobial effects of silver nanoparticles, *Nanomed Nanotechnol Biol Med* 3:95-101.

Klich, M.A. (2007). *Aspergillus flavus*: the major producer of aflatoxin, *Molecular Plant Pathology* 8(6): 713-22.

Knoll, S., R.F. Vogel and L. Niesen (2002). Idenfitication of *Fusarium graminearum* in cereal samples by DNA detection test strip, *Applied Microbiology.* 34: 144-148.

Krasovskii, V.I.V. and A. Karavanskii (2008). Surface plasmon resonance of metal nanoparticles for interface characterization, *Optical Memory and Neural Networks* (Information Optics) 17: 8–14.

Mah, C., I. Zolotukhin, T.J. Fraites, J. Dobson, C. Batich and B.J. Byrne (2000). Microsphere- mediated delivery of recombinant AAV vectors *in vitro* and *in vivo*, *Molecular Therapy* 1:239.

Mandal, D., M.E. Bolander, D. Mukhopadhyay, G. Sarkar and P. Mukherjee (2006). The use of microorganisms for the formation of metal nanoparticles and their application, *Applied Microbiology and Biotechnology* 69: 485-492.

Miller, J.D. (2002). Aspects of the ecology of *Fusarium graminearum* in cereals, *Advance Experimental and Medical Biology* 50: 19-27.

Mohanpuria, P., N.K. Rana and S.K. Yadav (2008). Biosynthesis of nanoparticles: technological concepts and future applications, *Journal of Nanoparticles Research* 10: 507-517.

Mukherjee, P., A. Ahmad, D. Mandal, S. Senapati, S.R. Sainkar and M. Khan (2001a). Bioreduction of Aucyl ions by the fungus, *Verticillum* species and surface trapping of the gold nanoparticles formed, *Angew Chem Int Ed* 40: 3585-3583.

Mukherjee, P., A., Ahmad, D. Mandal, S. Senapati, S.R. Sainkar, M.I. Khan, R. Parishcha, P.V. Ajaykumar, M. Alam, R. Kumar and M. Sastry (2001b). Fungus-mediated synthesis of silver nanoparticles and their immobilization in the mycelial matrix: A novel biological approach to nanoparticle synthesis, *Nano Letters* 1: 515-519.

Mukherjee, P., M. Roy, B. P. Mandal, G. K. Dey, P.K. Mukherjee, J. Ghatak, A.K. Tyagi and S.P. Kale (2008). Green synthesis of highly stabilized nanocrystalline silver

particles by a non-pathogenic and agriculturally important fungus *T. asperellum, Nanotechnology* 19: 075103 (7 pp).

O'Gorman, C.M., H.T. Fuller and P.S. Dyer (2009). Discovery of a sexual cycle in the opportunistic fungal pathogen *Aspergillus fumigatus*, *Nature* 457: 471-474

Rai, M., A. Yadav and A. Gade (2009). Silver nanoparticles as a new generation of antimicrobials, *Biotechnology Advances* 27: 76-83.

Rai, M.K and R.C. Rajak (1985). A Key to the identification of species of *Phoma* in culture, *J Econ Taxon Bot*, 7(3): 588-590.

Raj, K.S and K.K. Asha (2009). Nanotechnology in agriculture, *Trendz in Biotech*, 2: 27-28.

Riddin, T.L., M. Gericke and C.G. Whiteley (2006). Analysis of the inter- and extracellular formation of platinum nanoparticles by *Fusarium oxysporum* f. sp. *lycopersici* using response surface methodology, *Nanotechnology* 17: 3482-3489.

Sadowski, Z., I.H. Maliszewska, B. Grochowalska, I. Polowczyk and T. Kożlecki (2008). Synthesis of silver nanoparticles using microorganisms, *Materials Science-Poland* 26: 419-424.

Samson, R.A., J. Houbraken, R.C. Summerbell, B. Flannigan and J.D. Miller (2001). Common and important species of fungi and actinomycetes in indoor environments. In: Microogranisms in Home and Indoor Work Environments. New York: Taylor and Francis. pp. 287–292.

Sanghi, R. and P. Verma (2009). Biomimetic synthesis and characterisation of protein capped silver nanoparticles, *Bioresource Technology* 100: 501-504.

Sastry, M., A. Ahmad, M.I. Khan and R. Kumar (2003). Biosynthesis of metal nanoparticles using fungi and actinomycete, *Current Science* 85:162-170.

Schuster, E., N. Dunn-Coleman, J.C. Frisvad and P.W. Van Dijck (2002). On the safety of *Aspergillus niger*-a review, *Applied Microbiology and Biotechnology* 59 (4-5): 426–35.

Seifert, K. (1996). *Fusarium* interactive key. *Agriculture and Agri food Canada,* pp 1-30.

Senapati, S., D. Mandal, A. Ahmad, M. I. Khan, M. Sastry and R. Kumar (2004). Fungus mediated synthesis of silver nanoparticles: a novel biological approach, *Indian Journal of Physics and Proceedings of the Indian Association for the Cultivation of Science-Part A* 78A: 101-105.

Sharma, V.K., R.A. Yngard and Y. Lin (2009). Silver nanoparticles: Green synthesis and their antimicrobial activities, *Advanced in Colloid and Interface Science* 145: 83-96.

Shahverdi, A.R., A. Fakhimi, H.R. Shahverdi and S. Minanian (2007). Synthesis and effect of silver nanoparticles on the antibacterial activity of different antibiotics against *S. aureus* and *E. coli*, *Nanomed* 3:168-171.

Shen, H.D., H. Chou, M.F. Tam, C.Y. Chang, H.Y. Lai and S.R. Wang (2003). Molecular and immunological characterization of Pench 18, the vacuolar serine protease major allergen of *Penicillium chrysogenum*, *Allergy* 58: 993-1002.

Sondi, I and S.B. Sondi (2004). Silver nanoparticles as antimicrobial agents a care study on *E-coli* as a model for Gram-negative bacteria, *Journal of Colloid and Interface Science* 275:117-182.

Tan, Y., Y. Wang, L. Jiang and D. Zhu (2002). Thiosalicylic acid-functionalized silver nanoparticles synthesized in one-phase system, *Journal of Colloid and Interface Science* 249: 336-345.

Van der Aa, H.A., M.E. Noordeloos and J. de Gruyter (1990). Species concepts in some larger genera of the Coelomycetes, *Studies in Mycology* 32: 3-19

Vigneshwaran, N., A.A. Kathe, P.V. Varadarajan, R.P. Nachane and R.H. Balasubramanya (2006). Biomimetics of silver nanoparticles by white rot fungus, *Phaenerochaete chrysosporium*, *Colloids and Surfaces B: Biointerfaces* 53: 55-59.

Vigneshwaran, N., N.M. Ashtaputre, P.V. Varadarajan, R. P. Nachane, K. M. Paralikar and R.H. Balasubramanya (2007). Biological synthesis of silver nanoparticles using the fungus A*spergillus flavus, Materials Letters* 61: 1413-418.

Zare, R. and W. Gams (2001). A revision of *Verticillium* sect. *Prostrata*. III. Generic classification, *Nova Hedwigia* 72. 329-337.